

MIT Open Access Articles

*Strong interlayer charge transfer due to exciton condensation
in an electrically isolated GaAs quantum well bilayer*

The MIT Faculty has made this article openly available. **Please share**
how this access benefits you. Your story matters.

Citation: Jang, Joonho, Yoo, Heun Mo, Pfeiffer, LN, West, KW, Baldwin, KW et al. 2021. "Strong interlayer charge transfer due to exciton condensation in an electrically isolated GaAs quantum well bilayer." Applied Physics Letters, 118 (20).

As Published: 10.1063/5.0049595

Publisher: AIP Publishing

Persistent URL: <https://hdl.handle.net/1721.1/141423>

Version: Final published version: final published article, as it appeared in a journal, conference proceedings, or other formally published context

Terms of use: Creative Commons Attribution 4.0 International license



Strong interlayer charge transfer due to exciton condensation in an electrically isolated GaAs quantum well bilayer

Cite as: Appl. Phys. Lett. **118**, 202110 (2021); <https://doi.org/10.1063/5.0049595>

Submitted: 06 March 2021 • Accepted: 29 April 2021 • Published Online: 21 May 2021

 Joonho Jang, Heun Mo Yoo, L. N. Pfeiffer, et al.



View Online



Export Citation



CrossMark

ARTICLES YOU MAY BE INTERESTED IN

[Impact of formation process on the radiation properties of single-photon sources generated on SiC crystal surfaces](#)

Applied Physics Letters **118**, 204005 (2021); <https://doi.org/10.1063/5.0048772>

[Ultrawide bandgap semiconductors](#)

Applied Physics Letters **118**, 200401 (2021); <https://doi.org/10.1063/5.0055292>

[Origin of defect luminescence in ultraviolet emitting AlGaIn diode structures](#)

Applied Physics Letters **118**, 202101 (2021); <https://doi.org/10.1063/5.0047021>

Lock-in Amplifiers
up to 600 MHz



Zurich
Instruments



Strong interlayer charge transfer due to exciton condensation in an electrically isolated GaAs quantum well bilayer

Cite as: Appl. Phys. Lett. **118**, 202110 (2021); doi: [10.1063/5.0049595](https://doi.org/10.1063/5.0049595)

Submitted: 6 March 2021 · Accepted: 29 April 2021 ·

Published Online: 21 May 2021





View Online



Export Citation



CrossMark

Joonho Jang,^{1,2,3,a)}  Heun Mo Yoo,¹ L. N. Pfeiffer,⁴ K. W. West,⁴ K. W. Baldwin,⁴ and Raymond C. Ashoori^{1,a)} 

AFFILIATIONS

¹Department of Physics, Massachusetts Institute of Technology, Cambridge, Massachusetts 02139, USA

²Department of Physics and Astronomy, and Institute of Applied Physics, Seoul National University, Seoul 08826, South Korea

³Center for Correlated Electron Systems, Institute for Basic Science, Seoul 08826, South Korea

⁴Department of Electrical Engineering, Princeton University, Princeton, New Jersey 08544, USA

^{a)} Authors to whom correspondence should be addressed: joonho.jang@snu.ac.kr and ashoori@mit.edu

ABSTRACT

We introduce a design of electrically isolated “floating” bilayer GaAs quantum wells (QW), in which application of a large gating voltage controllably and highly reproducibly induces charges that remain trapped in the bilayer after removal of the gating voltage. At smaller gate voltages, the bilayer is fully electrically isolated from external electrodes by thick insulating barriers. This design permits full control of the total and differential densities of two coupled 2D electron systems. The floating bilayer design provides a unique approach for studying systems inaccessible by simple transport measurements. It also provides the ability to measure the charge transfer between the layers, even when the in-plane resistivities of the 2D systems diverge. We measure the capacitance and inter-layer tunneling spectra of the QW bilayer with independent control of the top and bottom layer electron densities. Our measurements display strongly enhanced inter-layer tunneling current at $\nu_T = 1$, a signature of exciton condensation of a strongly interlayer-correlated bilayer system. With fully tunable densities of individual layers, the floating bilayer QW system provides a versatile platform to access previously unavailable information on the quantum phases in electron bilayer systems.

© 2021 Author(s). All article content, except where otherwise noted, is licensed under a Creative Commons Attribution (CC BY) license (<http://creativecommons.org/licenses/by/4.0/>). <https://doi.org/10.1063/5.0049595>

Weakly coupled quantum Hall (QH) bilayer systems display a variety of exotic phases as the filling factor of the two layers varies.^{1–3} Under quantizing magnetic fields, decreasing the separation distance of two layers to become comparable to the mean interparticle spacing can drive the double layer system into phases not possible in single layers.^{4–6} When the individual layers are in strongly intralayer correlated states such as fractional quantum Hall phases, the additional interlayer coupling can play a non-trivial role that modifies the properties of the phases or even results in totally new ground states of the coupled 2D system. There are many theoretical proposals for non-trivial QH phases in such vertically coupled systems, including Pfaffian, Halperin, and exciton condensed phases.^{7–10}

The exciton condensate is an interlayer-coherent phase that shows dramatic macroscopic quantum phenomena, such as Josephson-like interlayer tunneling, quasiparticle tunneling, and perfect Coulomb drag, as observed in GaAs quantum wells (QW) bilayers and graphene bilayers.^{1,11–15} The interlayer interaction has an energy scale of E_c

$= 1/4\pi\epsilon d$ and competes with an intralayer Coulomb interaction of energy $E_b = 1/4\pi\epsilon l_B$, where d is the interlayer distance between the two layers and l_B is the magnetic length. As d/l_B decreases, the interlayer interaction starts to dominate over the intralayer interaction, favoring the formation of the interlayer correlated phases. The existence of the condensate phase depends critically on the ratio d/l_B , and experimenters have reported condensate phases at total filling factor $\nu_{tot} = 1$ ($\nu = 1/2$ in each layer) in samples with d/l_B smaller than 1.8, in the limit of weak interlayer tunnel coupling.^{4,16,17} In this picture, an interlayer bias voltage plays a role of pseudospin Zeeman energy for bilayer charge polarization.

In most previous experiments with bilayer QWs, charge carriers were induced by doping from top and bottom of the layers and one eventually needed to make Ohmic contacts for transport measurements.^{2,18} Specifically, the characteristic interlayer Josephson tunneling effect has been observed only with separate Ohmic contacts to individual layers. With such a sample design, in-plane and contact resistances

make high frequency measurements difficult, and it becomes impossible to make tunneling measurements when the longitudinal conductivity drops to zero. We instead use a contactless measurement scheme that functions independently of the conductivity of the layers. We electrically isolate the system of interest, a bilayer QW, in between top and bottom insulating barriers and introduce charge carriers via a controlled leakage over the barriers by applying large bias voltages, and we find that the charge carriers persist in the double well system for long periods of time (hours or days) after the removal of the large bias. In this way, we are able to control the individual layer densities while monitoring the interlayer charge transfer without electrical Ohmic contacts by detecting the displacement fields generated by interlayer-moving charges.

In this article, we present our contactless and electrically isolated design approach of a bilayer QW with fully tunable top and bottom layer densities. Our results show that the exciton condensation occurs in the isolated bilayer device. This design, along with capacitive pulsed tunneling spectroscopy¹⁹ permits contactless measurement of the tunneling current along with direct wide-bandwidth probing of the sample needed for study of quantum coherence.

In Figs. 1(a) and 1(b) the device schematic and the profile of the wafer (wafer id# pf-3.21.16) used in the measurements are shown. The bilayer is composed of two 18 nm GaAs QWs separated by a 6 nm Al_{0.8}Ga_{0.2}As barrier. Thick barriers of Al_{0.323}Ga_{0.677}As and Al_{0.8}Ga_{0.2}As isolate the QWs from the external top and bottom electrodes (n-dope GaAs). The wafer is etched by photo-lithography to

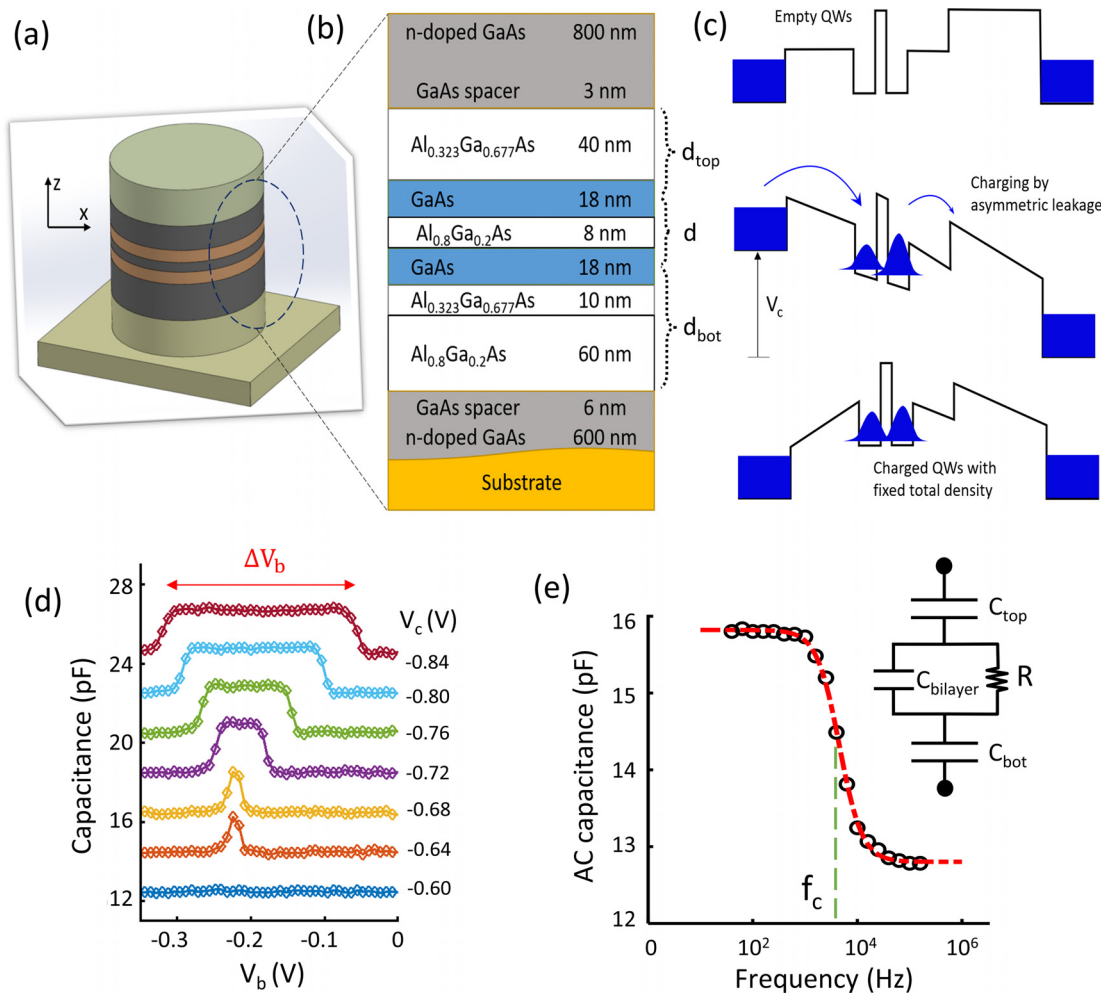


FIG. 1. Sample design and means for controlling total and differential density. (a) Schematic of a cylindrically etched device. (b) The wafer growth profile used in this work. The GaAs QWs of 18 nm width are tunneling-coupled to each other and form a QW bilayer. (c) Sequence of charging the bilayer system. An initially empty bilayer is charged by first inducing leakage current over the structure and capturing the charges in the bilayer. (d) Capacitance measured at 13 Hz as a function of V_b at various values of V_c used in the charging sequence of (c). Evidenced by the range of the high capacitance (red arrow), the amount of the total charge in the system grows with the increasing magnitude of V_c . Curves are shifted for clarity. (e) A frequency dependent capacitance measurement shows a roll-off behavior with the frequency ($f_c = 1/2\pi RC_{bilayer}$) proportional to the strength of interlayer charge transfer conductance ($S_{in} = 1/R$). The red dotted line is a fit to the frequency response function of the effective circuit in the inset.

define a cylindrical mesa of 150 μm -diameter and 1.5 μm -height vertical device. The top and bottom electrodes are contacted to the external measurement setups. A capacitance bridge and HEMT amplifiers are used to enhance the sensitivity of the measurements in cryogenics environment.^{19,20}

The conduction band edge of the barriers, which determines the potential profile for induced electrons, is controlled by the Al content of $\text{Al}_x\text{Ga}_{1-x}\text{As}$. The barriers have an asymmetric profile in top and bottom sides of the QWs by design so that electrons can accumulate in the bilayer when a large voltage bias V_c is applied. In Fig. 1(c), a sequence of charging the bilayer system is shown. The sample develops a DC leak current at V_c lower than -0.85 V and larger than 1.25 V. However, for V_c between -0.6 V and -0.85 V, although there is no DC leak current measured within our measurement resolution of ~ 10 pA, the measurements in Fig. 1(d) imply that the charges are trapped in the bilayer system, probably via a leak over one of the barriers. After waiting for 30 s with the voltage applied, the amount of trapped charges seems to saturate. We find that we can consistently and precisely set the amount of this remnant charge by controlling the value of V_c that we apply. The barriers are sufficiently thick to hold the induced charges in the bilayer system once V_c is removed: total density of the trapped charges changes less than 1% after 10 h at 4 K, whereas the measurement time for a fixed total density is typically within 10 min. Then, a smaller bias voltage V_b is used to control the density imbalance between the top and bottom QWs. Thus, with combinations of V_c and V_b , the individual densities of the two QWs are independently tunable. Note that the range of bias voltage (V_b) is maintained much smaller than that of V_c to prevent charges in the electrode or in the DQW from undergoing Fowler-Nordheim tunneling through one of the thick barriers, in which case the total charges in the bilayer can inadvertently change.

We designed our device structure to produce high mobility 2D electron systems; there is no doping present near the QWs and after charging the double-well system with electrons. Upon removing V_c , the bilayer system remains electrically well isolated without any Ohmic contacts from the external electrodes. To study charge transfer between the two layers embedded in the sample without contacts, we employ capacitance measurements and pulsed tunneling spectroscopy. For capacitance measurements, in addition to the DC bias voltages, we apply sinusoidal voltages with a fixed frequency and measure capacitive response between the electrodes using a home-made cryogenic capacitance bridge and HEMT amplifiers to study interlayer charge transfer. For tunneling spectroscopy, we use a contactless pulsed tunneling method, applying a sudden voltage step from external electrodes and remotely sense the electric field emanating from charges moving in-between layers via the HEMT amplifiers to measure interlayer tunneling spectra.^{19,20}

Precise determination of the total and differential density requires accurate measurements of capacitance of the device. We define total density $n_{\text{tot}} = n_1 + n_2$ and differential density $n_d = n_1 - n_2$, where n_1 and n_2 are the densities of top QW and bottom QWs, respectively. Once the total density of electrons in the bilayer system is fixed by the charging method described in Fig. 1(c), we can vary V_b to partition the remnant electron density between the wells, up to full depletion of either one of the QW layers. In Fig. 1(d), we plot capacitance data measured at quasi-DC limit of $f = 13$ Hz at various charging voltages V_c . To understand the data in Fig. 1(d), the sample is modeled as the

schematic circuit in the inset of Fig. 1(e). Here, considering only geometrical factors, C_{top} , C_{bilayer} , and C_{bot} are capacitances given by the vertical distances d_{top} , d , and d_{bot} as indicated in Fig. 1(b). When charges cannot move between QWs, i.e., in the limit of very large R , the measured capacitance would be the total capacitance of the three capacitances in series, resulting in the low capacitance values. This corresponds to the case that either one of the QWs is depleted or incompressible by applying V_b . On the other hand, when charges are allowed to move between the QWs, i.e., in the limit of small R , the capacitance is only given by C_{top} and C_{bot} in series, which accounts for the high capacitance values. This analysis quantitatively explains the data and identifies the central region of higher capacitance (ΔV_b) as the case that both QWs are charged and compressible, where the interlayer charge transfer is mainly responsible for the increase in the capacitance. As the total density increases with a larger magnitude of V_c , the central region (ΔV_b) becomes wider because more total charges in the system require larger positive or negative V_b to deplete either top or bottom QW. The data are consistent with independent control of the densities of two layers through changing V_b and V_c .

In the region of high capacitance, if we increase the measurement frequency, the measured value for capacitance shows a roll-off behavior with the characteristic frequency, f_c , as in Fig. 1(e). These frequency dependent capacitance (or AC capacitance) data yield information about the rate of charge movement between QW layers. In the zero-frequency limit, the capacitance measures thermodynamic charge-polarizability of the bilayer but, as the frequency increases, the measured capacitance falls because the interlayer charge transfer cannot keep up with the AC excitation due to finite interlayer tunneling conductivity. If we parameterize the interlayer charge transfer rate using a resistance R of an effective circuit diagram representing the device in the inset, f_c is given by $1/2\pi RC_{\text{bilayer}}$, where C_{bilayer} is the geometric capacitance of the bilayer.

In Fig. 2(a), the capacitance measured at 13 Hz as a function of V_b and V_c displays a clear signature of density control in an applied magnetic field. With increasing perpendicular magnetic fields, Landau levels form. Because filled Landau levels cannot charge due to energy gaps, we observe stripes of a suppressed capacitance when the Landau levels are full. The data visualize the densities of individual QWs being independently tunable by our method and provide straight-forward assignment of filling factors ($\nu = nh/eB$) to top and bottom QWs for the incompressible stripes, and they are denoted in the figure. At magnetic fields at and above 6 T, we observe that visible incompressible stripes and areas appear at fractional filling factors such as $1/3$, demonstrating that the electrically floating contactless design offers a versatile platform for studying the coupled systems of two single-layer QH phases.

We focus in the rest of this paper on the exciton condensed phase.^{1,11,12} When we increase the frequency of the capacitance measurement to 100 kHz, charge transfer is suppressed except for the regions where the interlayer charge transfer is comparably faster. As discussed above, if the characteristic frequency f_c is much smaller than the measurement frequency f , the AC capacitance signal would become strongly suppressed. First of all, for $B = 0$ T, the thin line of high interlayer charge transfer stands out [Fig. 2(a)], and this line corresponds to the equal densities of the two QWs; here, the conduction band edge and the energy dispersion of the two layers match, so that momentum conservation for interlayer tunneling is well satisfied,

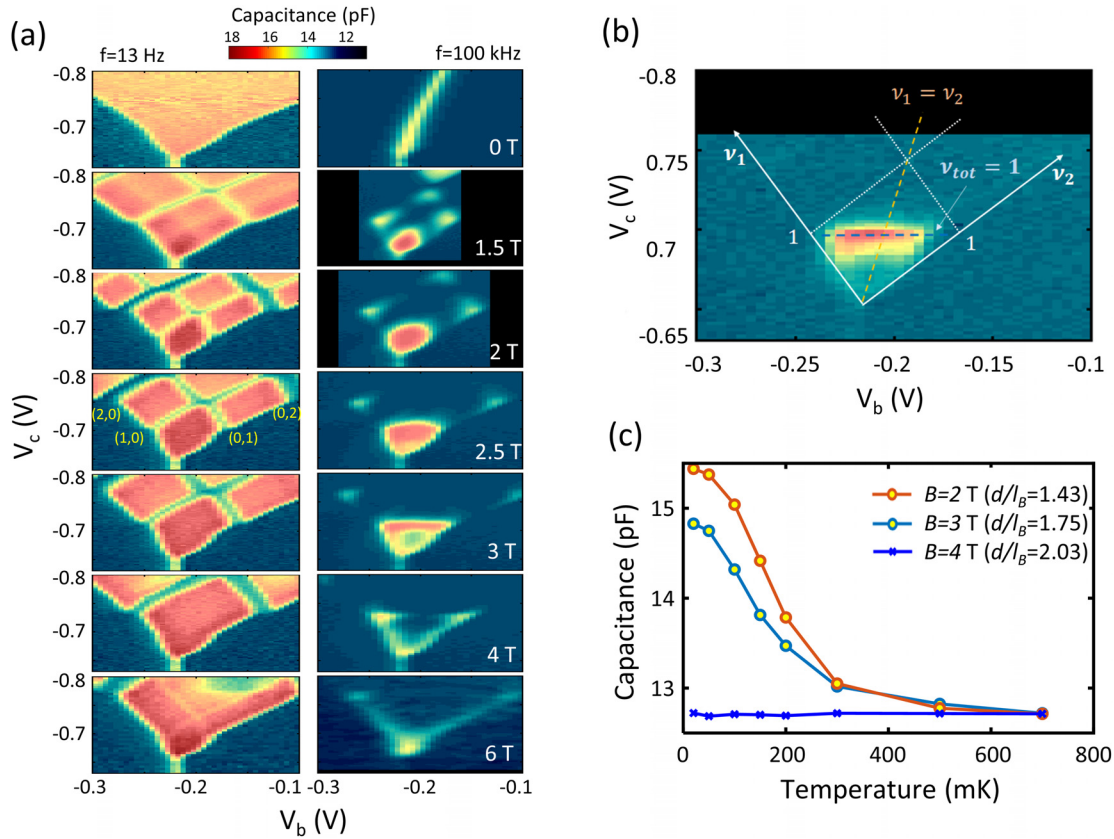


FIG. 2. Magnetic field and frequency dependence of AC capacitance measurements. (a) At base temperature of 20 mK, AC capacitances are plotted as a function of charging voltage (V_c) and bias voltage (V_b), at various magnetic fields and two different frequencies. The data measured at 13 Hz, which represent the quasi-DC limit of the capacitance of the sample, well visualize the densities of individual QWs being independently tunable by our method. The interlayer charge transfer rate is fast at certain filling factors due to the increased correlation of the top and bottom layers. (b) AC capacitance measured at $f = 1$ MHz and $B = 2.5$ T. Total and individual filling factors (ν_{tot} , ν_1 , ν_2) are denoted. At the total filling factor of 1 (dotted horizontal line), the very high interlayer conductivity signals the formation of the exciton condensation. (c) AC capacitance measured at $\nu_t = 1/2$, $\nu_b = 1/2$ with $f = 100$ kHz strongly increases at low temperature when $d/l_B < 1.8$. This temperature dependence suggests enhanced interlayer charge transfer as a result of the exciton condensation.

leading to fast interlayer tunneling.^{19,20} However, upon application of magnetic fields, Landau quantization modifies the condition for the momentum conservation and leads to the appearance of multiple patches of high capacitance. It is well known that Coulomb interaction between electrons creates a Coulomb gap at the Fermi level^{21–23} near non-integer filling factors and leads to an exchange gap around odd integer filling factors, suppressing tunneling near zero bias (i.e., Fermi level).¹⁸ Consequently, we attribute the small patches of fast charge transfer in 100 kHz data as a consequence of the Coulomb gap and the exchange gap disappearing near even integer filling factors.

However, noticeably at $B = 2.5$ T and 3 T, the signal becomes very strong along the line that corresponds to $\nu_T = 1$, suggestive of a strongly correlated top and bottom QH phase. The signal disappears for higher magnetic fields at 4 and 6 T. In Fig. 2(b), we observe that, for $B = 2.5$ T, the AC capacitance (a measure of interlayer charge transfer rate) at $\nu_T = 1$ remains high even at $f = 1$ MHz, the highest frequency in our capacitance measurements. We attribute this ultra-fast interlayer charge transfer to very high zero-bias tunneling conductivity as a consequence of the formation of an exciton condensed phase

in the bilayer QW system. This fast interlayer charge transfer suggests the presence of Josephson tunneling of the emergent interlayer coherent phase.⁴ Because the AC voltage amplitude applied between the QWs for the capacitance measurements is only $100 \mu\text{V}$, the signals at a very high frequency likely arise from the interlayer zero-bias conductivity peak, such as the nearly dissipationless Josephson current of a bilayer exciton condensate.¹⁶ Furthermore, as shown in Fig. 2(c), signals have a strong temperature dependence, and the feature only appears below 300 mK with $d/l_B \leq 1.8$, consistent with previous reports.^{16,17}

To confirm the picture, we performed the time-resolved tunneling measurements of the interlayer charge transfer in Fig. 3. We used square-shaped excitations on the external electrodes and measured interlayer charge transfer over a tunneling barrier in a time domain, following the techniques described in previous studies.^{19,20} When the spectrum is measured at $B = 2.5$ T and $T = 20$ mK, the tunneling conductivity is observed to be strongly peaked near zero tunneling voltage. However, when temperature is increased to 700 mK, the peak becomes significantly suppressed. Increasing the magnetic field rather

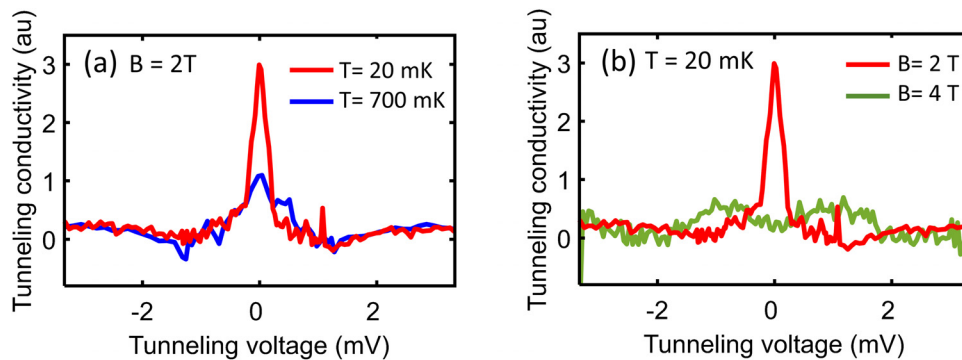


FIG. 3. Tunneling spectra of an exciton condensed phase. (a) Time-resolved tunneling spectra measured at $B = 2\text{ T}$ with $T = 20\text{ mK}$ (red) and 700 mK (blue). (b) Spectra measured at $T = 20\text{ mK}$ with $B = 2\text{ T}$ (red) and 4 T (green). Note that the red curve is the same in (a) and (b) for better comparison. The strong peak near zero tunneling bias suggests Josephson effect of an interlayer coherent exciton phase.

than the temperature also affects the signal. The data at 4 T and 20 mK show that the strong peak disappears, while the typical spectral features of the aforementioned Coulomb gap near zero tunneling bias remain visible [Fig. 3(b)]. Thus, the tunneling spectra give fully consistent pictures with the AC capacitance data of the Josephson tunneling peak. We note that the width of the tunneling peak ($\sim 100\text{ }\mu\text{eV}$) is wider than the one reported in Ref. 16. Possible reasons could be more disorders in the current sample or a thin tunneling barrier making Δ_{SAS} two orders of magnitude larger.

One of the main advantages of this electrically isolated “floating” bilayer design becomes more apparent when considering the range of differential densities over which we can observe the enhanced interlayer charge transfer of an exciton phase. Unlike previous transport measurements that showed evidence of this exciton condensation and its Josephson-like tunneling effects,^{16,17} our samples are designed to induce and measure vertical charge transfer independent of the lateral conductivities of individual 2D systems. This capability can be quite crucial when tuning densities of 2D systems in regimes of highly incompressible QH phases.²⁴ We can perform experiments with large differential density of the QW bilayer; i.e., the densities (and thus filling factors) of two QWs can be tuned in a wide range independently, even to incompressible low conductive regions, while maintaining the accuracy of the measurements. Perhaps more importantly, these measurements can be done without direct external contacts to any of these layers, eliminating any chance that the measurements are affected by extrinsic effects, so that a delicate quantum phase, such as the exciton condensation phase, is best preserved to provide evidence as a bulk phenomenon and a thermodynamic ground state. The strong signal at high frequency, such as shown in Fig. 2(b), in a wide range of differential density along the dotted line of $\nu_T = 1$ indicates the robust formation of the condensate in our sample. More detailed study of the exciton condensates in large density imbalance, and their tunneling spectra will be presented elsewhere.²⁵

Strongly interacting 2D bilayers provide a versatile platform to engineer rich physics as parameters for interlayer and intralayer interactions are tuned. The sample design and technique presented in this paper allow control of the parameters in a wide range and lead to the realization of the exciton condensation, demonstrating as a promising direction to control and detect the quantum phases of bilayer in

electrically isolated devices. Considering recent progress in 2D material systems such as graphene and transition metal dichalcogenides toward fabricating high quality bilayers, our unique approach presented here will be found to be useful.^{26,27}

The authors declare no conflict of interest.

The work at MIT was supported by the Basic Energy Sciences Program of the Office of Science of the U.S. Department of Energy through Contract No. FG02-08ER46514 and by the Gordon and Betty Moore Foundation through Grant No. GBMF2931. The work at Princeton was by the Gordon and Betty Moore Foundation’s EPiQS Initiative, Grant No. GBMF9615 to L. N. Pfeiffer and by the National Science Foundation MRSEC Grant No. DMR 1420541. The work at SNU was supported by the Creative-Pioneering Researchers Program of Seoul National University, the POSCO Science Fellowship of POSCO TJ Park Foundation, and the National Research Foundation (NRF) of Korea (Grant Nos. 2020R1A5A1016518 and 2019R1C1C1006520).

DATA AVAILABILITY

The data that support the findings of this study are available from the corresponding author upon reasonable request.

REFERENCES

- ¹Z. Ezawa and A. Iwazaki, “Quantum Hall liquid, Josephson effect, and hierarchy in a double-layer electron system,” *Phys. Rev. B* **47**, 7295 (1993).
- ²M. Shayegan, H. C. Manoharan, Y. W. Suen, T. S. Lay, and M. B. Santos, “Correlated bilayer electron states,” *Semicond. Sci. Technol.* **11**, 1539 (1996).
- ³J. P. Eisenstein and A. H. Macdonald, “Bose-Einstein condensation of excitons in bilayer electron systems,” *Nature* **432**, 691 (2004).
- ⁴D. Nandi, A. D. K. Finck, J. P. Eisenstein, L. N. Pfeiffer, and K. W. West, “Exciton condensation and perfect Coulomb drag,” *Nature* **488**, 481 (2012).
- ⁵V. Pellegrini, A. Pinczuk, B. S. Dennis, A. S. Plaut, L. N. Pfeiffer, and K. W. West, “Evidence of soft-mode quantum phase transitions in electron double layers,” *Science* **281**, 799 (1998).
- ⁶B. Skinner, “Chemical potential and compressibility of quantum Hall bilayer excitons,” *Phys. Rev. B* **93**, 085436 (2016).
- ⁷E. Fradkin, “A Chern-Simons effective field theory for the Pfaffian quantum hall state,” *Nucl. Phys. B* **516**, 704 (1998).
- ⁸B. I. Halperin, P. A. Lee, and N. Read, “Theory of the Half-filled Landau level,” *Phys. Rev. B* **47**, 7312 (1993).

- ⁹V. M. Apalkov and T. Chakraborty, "Stable Pfaffian state in bilayer graphene," *Phys. Rev. Lett.* **107**, 186803 (2011).
- ¹⁰W. Zhu, Z. Liu, F. D. M. Haldane, and D. N. Sheng, "Fractional quantum Hall bilayers at half filling: Tunneling-driven non-abelian phase," *Phys. Rev. B* **94**, 245147 (2016).
- ¹¹S. Murphy, J. Eisenstein, G. Boebinger, L. Pfeiffer, and K. West, "Many-body integer quantum Hall effect: Evidence for new phase transitions," *Phys. Rev. Lett.* **72**, 728 (1994).
- ¹²E. Tutuc, M. Shayegan, and D. Huse, "Counterflow measurements in strongly correlated GaAs Hole bilayers: Evidence for electron-hole pairing," *Phys. Rev. Lett.* **93**, 1 (2004).
- ¹³D. Zhang, J. Falson, S. Schmult, W. Dietsche, and J. H. Smet, *Phys. Rev. Lett.* **124**, 246801 (2020).
- ¹⁴J. I. A. Li, T. Taniguchi, K. Watanabe, J. Hone, and C. R. Dean, "Excitonic superfluid phase in double bilayer graphene," *Nat. Phys.* **13**, 751 (2017).
- ¹⁵X. Liu, K. Watanabe, T. Taniguchi, B. I. Halperin, and P. Kim, "Quantum Hall drag of exciton condensate in graphene," *Nat. Phys.* **13**, 746 (2017).
- ¹⁶I. Spielman, M. Kellogg, J. Eisenstein, L. Pfeiffer, and K. West, "Onset of interlayer phase coherence in a bilayer two-dimensional electron system: Effect of layer density imbalance," *Phys. Rev. B* **70**, 1 (2004).
- ¹⁷L. Tiemann, Y. Yoon, W. Dietsche, K. von Klitzing, and W. Wegscheider, "Dominant parameters for the critical tunneling current in bilayer exciton condensates," *Phys. Rev. B* **80**, 1 (2009).
- ¹⁸K. Muraki, T. Saku, Y. Hirayama, N. Kumada, A. Sawada, and Z. F. Ezawa, "Interlayer charge transfer in bilayer quantum Hall states at various filling factors," *Solid State Commun.* **112**, 625 (1999).
- ¹⁹O. E. Dial, R. C. Ashoori, L. N. Pfeiffer, and K. W. West, "High-resolution spectroscopy of two-dimensional electron systems," *Nature* **448**, 176 (2007).
- ²⁰J. Jang, H. M. Yoo, L. N. Pfeiffer, K. W. West, K. W. Baldwin, and R. C. Ashoori, "Full momentum- and energy-resolved spectral function of a 2D electronic system," *Science* **358**, 901 (2017).
- ²¹J. P. Eisenstein, T. J. Gramila, L. N. Pfeiffer, and K. W. West, "Probing a two-dimensional Fermi surface by tunneling," *Phys. Rev. B* **44**, 6511 (1991).
- ²²R. Ashoori, H. Stormer, J. Weiner, L. Pfeiffer, S. Pearton, K. Baldwin, and K. West, "Single-electron capacitance spectroscopy of discrete quantum levels," *Phys. Rev. Lett.* **68**, 3088 (1992).
- ²³J. Eisenstein, L. Pfeiffer, and K. West, "Coulomb barrier to tunneling between parallel two-dimensional electron systems," *Phys. Rev. Lett.* **69**, 3804 (1992).
- ²⁴J. Jang, B. M. Hunt, L. N. Pfeiffer, K. W. West, and R. C. Ashoori, "Sharp tunnelling resonance from the vibrations of an electronic Wigner crystal," *Nat. Phys.* **13**, 340 (2017).
- ²⁵H. Yoo, J. Jang, L. N. Pfeiffer, K. West, K. Baldwin, and R. C. Ashoori, "Coherent tunneling at large layer imbalance in the quantum Hall bilayer" (unpublished).
- ²⁶G. L. Yu, R. Jalil, B. Belle, A. S. Mayorov, P. Blake, F. Schedin, S. V. Morozov, L. A. Ponomarenko, F. Chiappini, S. Wiedmann, U. Zeitler, M. I. Katsnelson, A. K. Geim, K. S. Novoselov, and D. C. Elias, "Interaction phenomena in graphene seen through quantum capacitance," *Proc. Natl. Acad. Sci. U.S.A.* **110**, 3282 (2013).
- ²⁷Y. Cao, V. Fatemi, A. Demir, S. Fang, S. L. Tomarken, J. Y. Luo, J. D. Sanchez-Yamagishi, K. Watanabe, T. Taniguchi, E. Kaxiras, R. C. Ashoori, and P. Jarillo-Herrero, "Correlated insulator behaviour at Half-filling in magic-angle graphene superlattices," *Nature* **556**, 80 (2018).